Available online at www.sciencedirect.com

ScienceDirect

Proceedings of the Combustion Institute 38 (2021) 523–532

Proceedings of the Combustion Institute

www.elsevier.com/locate/proci

On the combustion and sooting behavior of standard and hydro-treated jet fuels: An experimental and modeling study on the compositional effects

M. Pelucchi [a], P. Oßwald [b,1], W. Pejpichestakul [a], A. Frassoldati [a], M. Mehl [a,*]

[a] *CRECK Modeling Lab, Department of Chemistry, Materials and Chemical Engineering "G. Natta", Politecnico di Milano, P.zza Leonardo da Vinci 32, 20133 Milano, Italy*

[b] *German Aerospace Center (DLR), Institute of Combustion Technology, Pfaffenwaldring 38-40, 70569 Stuttgart, Germany*

Received 7 November 2019; accepted 28 June 2020
Available online 16 September 2020

Abstract

In a context of growing level of environmental awareness, emission from aviation are the subject of increasing scrutiny. This situation poses important challenges because, due to safety, practical and economic factors, aero-transportation technologies are not likely to undergo rapid paradigm shifts. An area where important innovations are being introduced is fuel technology: fuels from alternative processes, potentially from renewable sources, offer the opportunity of limiting the carbon footprint of transportation, moreover, a better control on fuel quality can contribute to reducing emissions.

Hydro-treating of oil based fuels can reduce their sulfur and aromatic content promoting a cleaner combustion. In order to better understand the impact of hydro-treating on emissions of PAHs and soot from jet fuels, new speciation data covering oxidation intermediates and soot precursors were measured in a flow reactor for a standard jet fuel and its hydro-treated counterpart. Using a detailed kinetic mechanism and complex surrogate blends mimicking the composition of the real fuels, the speciation data from the flow reactor were simulated. Additionally, soot formation trends were calculated and compared with previously published data. Using the kinetic model, which is based on mechanistic principles, it was possible to separate the relative contribution of different processes and, for the fuel blends of interest, the role played by specific components in the PAHs and soot formation. The results obtained provide useful information towards more effective fuel formulation strategies and fuel blends modeling.

Keywords: Jet fuels; Kinetic modeling; Surrogate fuels; Flow reactor data; PAHs and soot

* Corresponding authors.
E-mail addresses: marco.mehl@polimi.it, patrick.osswald@dlr.de (M. Mehl).
[1] Patrick Osswald, Deutsches Zentrum für Luft- und Raumfahrt (DLR), Institute of Combustion Technology, Pfaffenwaldring 38–40, 70569 Stuttgart, Germany

https://doi.org/10.1016/j.proci.2020.06.353

1. Introduction

Emissions from the aviation sector are receiving increasing attention due to increased environmental awareness. This situation poses important challenges because, due to safety, practical and economic factors, aero-transportation technologies are not likely to undergo rapid paradigm shifts. An area where important innovations are being introduced is fuel technology: fuels from alternative processes, potentially from renewable sources, offer the opportunity of limiting the carbon footprint of transportation, moreover, a better control on fuel quality can contribute to reducing emissions.

A common step in the production of alternative jet fuels is the hydro-treating process: hydrotreatment of fuels from renewables is used to reduce their oxygen and to get rid of unsaturated molecules that affect negatively both the fuel oxidative stability and its propensity to form gums which are detrimental to fuel systems in aircrafts. Hydrotreating can also be applied to conventional fuels to reduce their sulfur and aromatic content, with beneficial effects on emissions control. In order to better understand the impact of hydro-treating on PAHs and soot emissions from jet fuels, a flow reactor equipped with a molecular beam mass spectrometer was used to measure the formation of soot precursors from a standard jet fuel and its hydrotreated counterpart and detailed chemistry calculations were performed to interpret and extend the results. Blends mimicking the real fuels were applied in combinations with the detailed kinetic mechanism to reproduce both the speciation data from the flow reactor and previously published soot data. The use of oxidation models based on fundamental chemistry allows to separate the relative contribution of different processes and, in the case of mixtures, of specific components to PAHs and soot production. This features allowed to design a targeted parametric study aimed at better define the role of mono- and di-aromatics on soot emissions from jet fuel combustion and to obtain insights that are useful for fuel formulation strategies and fuel blends modeling.

2. Experimental set up

Quantitative species profiles for a standard Jet A-1 fuel (A1) and its hydro-treated version (A1.3) have been measured in the DLR high temperature flow reactor [1] using a molecular beam mass (MBMS) spectrometer. These data provide useful information about the chemical evolution of the fuels along their combustion process and are valuable validation targets for the detailed chemical kinetic fuel models used in this work. Since comprehensive recent literature on the applied experimental setup is available [2–4], only a brief description is given here.

Table 1
Inlet conditions and H-content. 17.64 g/min Ar diluent added at all conditions.

Fuel		A1	A1.3
Hydrogen	[wt%]	14.022	14.428
Uncertainty (SD)	[wt%]	0.024	0.016
Fuel	[mg/min]	31.16	31.31
O_2 for $\phi = 0.8$	[mg/min]	132.60	134.00
O_2 for $\phi = 1.2$	[mg/min]	88.40	98.40

The system can be divided into two segments: first, the high temperature laminar flow reactor including gas supply and vaporizer system and second, a molecular beam mass spectrometry (MBMS) time-of-flight detection (TOF) system. The reactor exit is positioned to the sampling nozzle of the MBMS-TOF system and gas is sampled directly from the reactor outlet and transferred to the high-vacuum system of the TOF-MS.

The reactor itself features a ceramic tube (40 mm inner diameter, total length of 1497 mm). Premixed laminar flowing gasses are fed highly diluted (over 99% Ar) into the reactor to suppress significant heat release and a self-sustaining reaction. The fuels are pre-vaporized using a commercial system (Bronkhorst, CEM) with a pneumatically driven fuel supply equipped with a Coriolis flow meter (Bronkhorst, Mini Cori-Flow M12). All input streams are metered in high precision (accuracy ±0.5%) by Coriolis mass flow meters. Complete evaporation was ensured by the small fuel fraction and the low partial pressure needed (typically below 100 Pa). Conditions are designed to yield constant carbon flow at slightly rich ($\varphi = 1.2$) and lean ($\varphi = 0.8$) conditions respectively. The oxidizer (O_2) is adjusted according to the desired stoichiometry. For adjustment of the respective stoichiometry, the hydrogen content of the fuels was determined in high precision by low resolution pulsed NMR (ASTM D7171), heteroatoms are neglected and the corresponding carbon content is assumed as the remainder. The obtained H-content is summarized in Table 1 with the respective mass inlet flow conditions.

Gasses were sampled at the reactor exit, transferred to high vacuum (10^{-6} mbar) by a two-stage differential pumping system. Due to this rapid expansion chemical reactions are quenched immediately and the composition of the gas sample, including reactive species, is preserved. The species are detected by an electron impact (EI) time-of-flight (TOF) mass spectrometer (Kaesdorf, mass resolution $R = 3000$). The MBMS-TOF system is capable to determine the elemental composition of combustion intermediates within a C/H/O system. To avoid species fragmentation at the ionization process, soft electron energies are applied (10.6 eV). Additionally, a residual gas analyzer (RGA), i.e. a quadrupole mass spectrometer, was placed in the

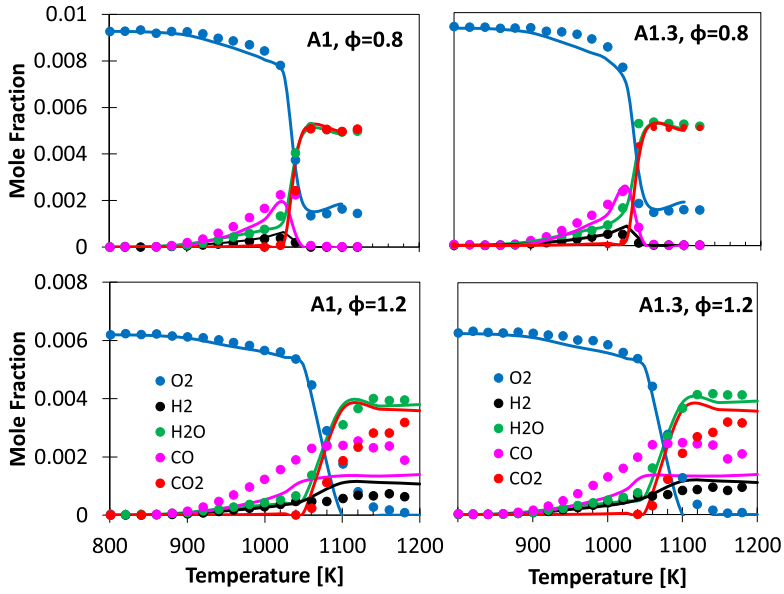

Fig. 1. Major species profiles (H_2, H_2O, O_2, CO_2, CO) measurement (Symbols) and simulation (Lines) . Left panels: A1, $\varphi = 0.8$ (top), $\varphi = 1.2$ (bottom). Right panels: A1.3, $\varphi = 0.8$ (top), $\varphi = 1.2$ (bottom).

ionization chamber (off beam) and operated at a higher electron energy (70 eV) allowing for tracking the major species simultaneously to the MBMS-TOF measurements. Details on the experimental setup, including schematic and its instrumentation may be found in previous publications [1,2].

The measurements were performed at constant inlet mass flow with a monotonically decreasing temperature ramp (−200 K/h) applied to the oven. The temperature range is chosen from 770 to 1200 K to cover the regime from unreacted fuel to full conversion to thermal equilibrium as it occurs in common combustion processes. Flow conditions are in the laminar regime for all temperatures and previous studies have successfully reproduced the experimental results applying a zero dimension (i.e. plug flow) kinetic model calculation [1,5] using a predefined temperature profile. Axial profiles for any oven temperature are known and can be used as boundary condition for the kinetic model simulations. Axial temperature profiles are provided in the Supplementary Material. Quantitative evaluation was performed following well established methods described in previous publications [1,6,7].

For the two fuels, the standard and the hydrotreated one (A1 and A1.3) at ϕ=0.8 and $\phi = 1.2$ a total number over 500 quantitative species profiles could be obtained and reported. Fig. 1 summarizes the major species (product and reactants) for all measurements. The two fuels exhibit similar behavior, a feature shared by several other aviation fuels and many pure constituents the technical fuels: the major species profiles are a close match to the ones measured in published [8,9] and unpublished works on similar fuels [10].

3. Kinetic model and surrogate formulation: the fuel model

This work aims at analyzing, experimentally and numerically, the combustion behavior of two full blend fuels. In order to capture the combustion behavior of these complex blends we adopted the CRECK kinetic model developed at Politecnico di Milano. Typically, jet fuels include 100 s of components from many classes (n-alkanes, isoalkanes, cycloid-alkanes, aromatics, di-aromatics) with a number of carbons in the C_7–C_{16} range [10]. The CRECK model accounts for the combustion chemistry of a variety of species relevant to aviation fuels, including C_{12} *n*- and isoparaffins, decalin, tri-methylbenzene, methyl-cyclohexane and α-methylnaphthalene, enabling the simulation of complex blends [11,12]. The modular structure of the CRECK model allows to seamlessly couple a discrete sectional soot formation model, also developed at CRECK [13–15]. The model thus obtained constitutes a suitable tool for the analysis of compositional effects on the formation of soot.

At the core of the kinetic models is the Aramco C_0–C_2 mechanism from Metcalfe et al. [16] and the C_3 subset from Burke et al. [17]. Minor updates from [18] have been incorporated in the C_0–C_1 chemistry. A discussion of the low- and high-temperature combustion mechanisms and of the

Table 2
Composition of jet fuel surrogates tested in this study.

Mole%	(A1)	(A1.3)	(A1-ND)	(A1.3-WD)
n-$C_{12}H_{26}$	20	21	21	21
Iso- $C_{12}H_{26}$	22	22	22	22
Iso- $C_{16}H_{34}$	8	10	8	8
Methyl-cyclohexane	21	28	22	28
Decalin	10	10	10	10
Tri-methylbenzene	17	9	17	9
α-methylnaphthalene	2	0	0	2
Molecular Weight (MW)	147.1	147.7	146.9	146.1
H/C Ratio	1.96	2.03	1.98	2.00

general principles used to represent heavier components can be found in Ranzi et al. [12]. Recent updates to mono-aromatic and poly-aromatic hydrocarbons are reported in [19,20]. The global high and low temperature mechanism, excluding the soot module, consists of 488 species and 17,193 reactions. For flames simulation, the low temperature chemistry can be excluded. Adding the soot module an overall mechanism of 451 species and 23,480 reactions is obtained. Both the models with thermodynamic and transport properties are reported in the Supplementary Material.

As mentioned, jet fuels are complex blends of 100 s of components and the CRECK model includes some of them, but not all. A common practice in the simulation of complex fuels is to adopt simpler mixtures, defined as surrogates, to emulate their properties. From a chemical standpoint, the key to a successful surrogate formulation is to choose a subset of fuel components that capture the relative content of specific moieties in the target fuel [21]. In this work, which focuses on the simulation of simple 1-D combustion systems, there were no constraints on the number of components to be used, therefore, an extended palette containing up to 8 components was defined. In order to better account for the distribution of molecular weights and moieties in the real fuel, more than one representative for each of the component classes were included. The combination of the fuel surrogate and of the kinetic model constitutes the fuel model.

The selection of the surrogate components and of their relative content is often treated as an optimization problem targeting compositional information, distillation curves, average molecular weight, H/C ratio, derived cetane number, etc. Since the focus of this work is on the compositional effects, and a detailed hydrocarbon analysis of the fuels performed at IFPEN through GC x GC technique was available [10], a direct approach where the fuel components types and quantity was closely matched was preferred. Table 2 summarizes the surrogate selection.

Two surrogates, one for fuel A.1 (the standard Jet A-1 fuel) and one for fuel A.1.3 (the hydro-treated fuel) were formulated based on the GCxGC analysis, weighting both the relative content of family of compounds and their molecular weight. Two representative species were included to represent the cyclic compounds and isoalkanes, the two most abundant families of fuel components. Notably, the hydro-treated fuel contains about the same amount of bicyclic alkanes (e.g. decalin) but significantly different amounts of single ring saturated species (e.g. methyl-cyclohexane). The difference is mainly resulting from the hydrogenation of the single ring aromatic species in the initial fuel. A minor compositional difference that have important implications, as explained later, is also the total absence of di-aromatic species (e.g. α-methylnaphthalene) in the hydro-treated fuel. The GCxGC data used to support the surrogate selection and the computed value of some relevant surrogate properties are available as Supplementary Material.

Two more surrogates were also formulated: one, labeled A1-ND, is a fuel containing the same amount of single ring aromatics as the standard A1, but without any di-aromatic species, the other, labeled A1.3-WD, is analogous to the hydro-treated fuel surrogate but with a 2 mol% α-methylnaphthalene added. These two surrogates do not correspond to any of the real fuel tested but, having intermediate compositional features between the two original surrogates, they allow to isolate in our computations the contribution of single and double rings fuel components on PAHs formation.

4. Results

The first step of this investigation is the analysis of the soot precursor measured in the DLR flow reactor.

Fig. 1 already introduced some modeling results. In general terms, it is possible to observe a good agreement between model and the measurements. The two fuels show similar reactivity in terms of major species profiles (Fig. 1), with some minor differences highlighted for intermediate and product species originating from the different compositions. The different hydrogen content clearly results in a ~20% difference in the

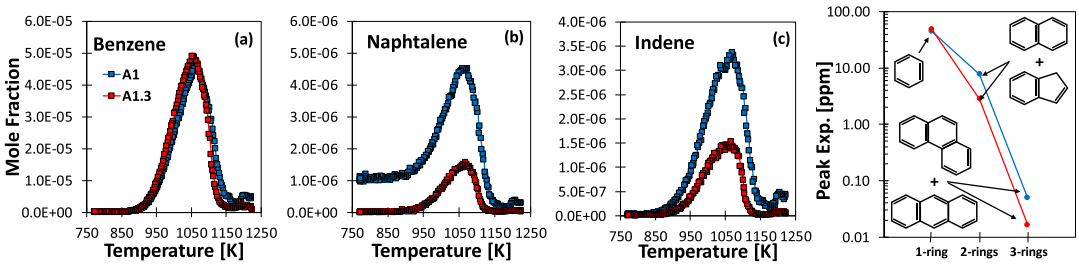

Fig. 2. Soot precursor species measured at rich conditions ($\Phi = 1.2$) for the tested fuels A1 (Hydrogen [wt%]=∼14.0, Table 1) and A1.3 (Hydrogen [wt%]=∼14.4, Table 1). Panel d) shows trend of cumulated peak concentrations of increasingly heavier PAHs.

asymptotic value of H_2. The same reason lies behind the difference in H_2O formation (∼10%). The model properly predicts the reactivity i.e. the temperature range of conversion for both stoichiometries. However the CO to CO_2 conversion at temperatures around 1100 K is not well reproduced at the $\varphi = 1.2$ condition. More specifically, in the predictions, the conversion of CO to CO_2 appears to be significantly faster, resulting in an under prediction of the CO peak. This issue is prevalent only at the mildly rich conditions and temperatures around 1100 K, after all the major oxidation and pyrolysis intermediates have already peaked. At this stage of the oxidation process the oxygen concentration is significantly lower and the OH production processes are less effective and, because of the relatively low temperature of the reactor, any external agent that favors their termination has a great impact on the CO/CO_2 rate of conversion. It is well documented that interactions with solid walls such as probing cones and reactor walls, as well as any non-ideality in the system (it should reminded that the plug flow assumption made in the calculation is a simplification of a more complex fluid-dynamics) can contribute to the local quenching (either chemical or thermal) of the reactive mixture [22]. It should be noted though, that the rate of fuel consumption up to 1100 K is very well captured and that all the major species relevant to the formation of soot are formed and mostly consumed in this early phase of the oxidation and are largely unaffected by this phenomenon.

Figure 2a, b and c, summarize some of selected soot precursor intermediate species: benzene (C_6H_6), indene (C_9H_8) and naphthalene ($C_{10}H_8$). Note that naphthalene is also a constituent of fuel A1 and therefore it starts with a non-zero concentration. Fig. 2d) highlights the differences in the peak amounts formed by the two fuels for aromatic species with increasing molecular weight. As can be expected, soot precursor species are more abundant for the A1 fuel, due to its higher aromatic content (or, in other terms, lower hydrogen content). This is consistent with previous results that point to the hydrogen content as a useful indicator of sooting propensity in technical combustors such as jet engines [23]. Interestingly, the trend here shown, indicates that both fuels form similar amounts of single ring aromatics, and the PAHs formation process starts differentiating only from double ring structures on. Indeed a correlation of single ring species and the Hydrogen content or the index of hydrogen deficiency [24] can be drawn for many fuels. The experimental examination of a large number fuels in the Jet A range at the same conditions as invigilated herein indicates a disproportionate impact of the fuels naphthalene content to the higher multi ring soot precursor species [10]. The detailed kinetic examination of a large number of fuels is beyond the scope of the Present work but the present example highlights the high value of detailed speciation data, which allow to isolate unexpected behaviors as the one just mentioned.

The next step is the validation of the proposed fuel models and the interpretation of the data. All the simulations performed in this work were carried out using the OpenSMOKE++ framework [25].

Intermediate species, however, are predicted properly. Fig. 3 compares experimental measurements and model simulations for the two main fuels analyzed in this study (fuel A1, the standard Jet A-1, and fuel A1.3, the hydro-treated fuel). It is worth noting that acetylene peak concretions are remarkably small at the investigated conditions and a second raise at high temperatures is observed at rich conditions. The raise of C_2H_2 at high Temperatures represents the onset of pyrolytic processes of the remaining hydrocarbons at rich conditions. This is seen for C_2H_2 for all fuels measured at these conditions and originates form small amounts of remaining C_2H_4. Details have been examined for very rich conditions [4]. Once again, deviation of the model prediction may be related to the limitations of the ideal plug flow assumption that predicts a complete C_2H_4 consumption (consistently with the enhanced CO to CO_2 conversion) while traces remain in the experiment. Prediction of C_2H_2 at the lean conditions is, however, in good agreement.

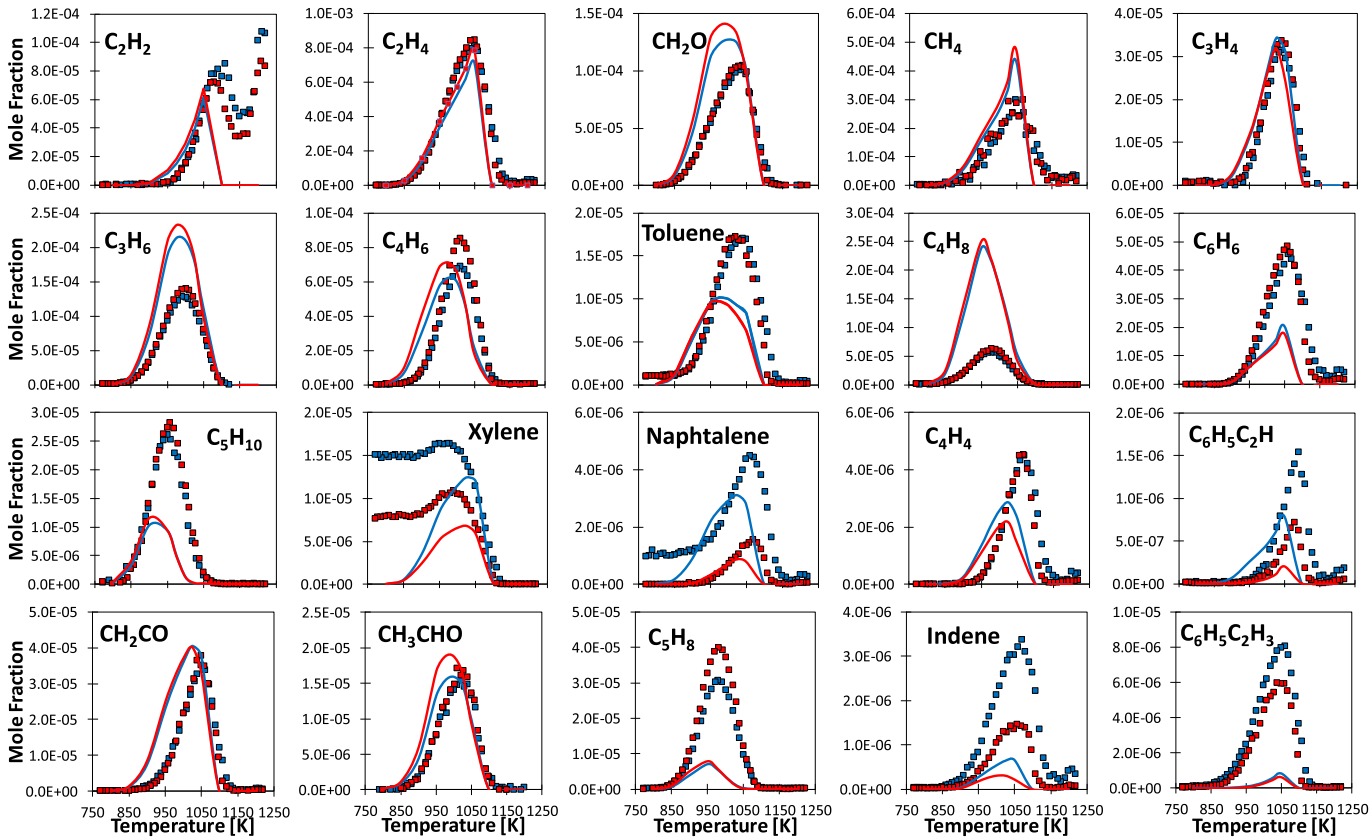

Fig. 3. comparison between experimental measurements and results from model simulations for major species (mole fraction > 1 ppm). $\varphi = 1.2$. Red: A1, blue: A1.3.

Very similar yields are observed for the remaining species (C_2H_4, CH_2O, CH_4, C_3H_4, C_3H_6, C_4H_8, C_5H_{10}, CH_2CO, CH_3CHO, C_4H_4, C_6H_6, toluene-C_7H_8), exception made for some mono-aromatic and poly-aromatic hydrocarbons. Indeed, significant differences can be observed for xylene, styrene, phenyl-acetylene, naphthalene and indene.

The fuel models (i.e. the combination of the kinetic and the surrogate models) reproduce correctly not only the onset of reactivity and its overall development, but also most of the differences observed experimentally between the two fuels, both qualitatively and quantitatively. Beside more or less significant deviations in terms of absolute concentration, which could be imputed to the simplified composition, the fuel models are capable of reproducing all the significant trends in a semi-quantitative, if not exact, manner. For instance, it is possible to reproduce features such as the similar amounts of benzene formed and the significant decrease in naphthalene, xylene, phenylacetylene and indene yields in the case of the hydrotreated jet fuel A1.3. Additional comparisons for the lean case (φ=0.8) are reported in the Supplementary Material showing similar of agreement.

Using the model, a rate of production analysis (ROPA) allowed to link the poly-aromatic species earlier discussed to the fuel components from which they originate. Fig. 4 summarizes the results by indicating which fuel species contribute the most to the formation of PAHs with increasing molecular weight.

The analysis showed how decalin, a bi-cyclic saturated species, plays an important role in the formation of 1 and, to a minor extent, 2 rings aromatic species, which are formed by partial decomposition and dehydrogenation reactions, but, do not contribute much to the formation of larger aromatics, since its oxidation is highly competitive with the pyrolytic pathways. On the other end, trimethylbenzene, the species representing the single ring aromatics in the fuel, sees its methyl groups oxidized to form benzene ring but it's also susceptible to growth reactions from additions on the stable benzylic radicals. The multiple methylations make tri-methylbenzene prone to the formation of multi-ring species. Finally, the di-aromatic ring present in the A1 fuel is too stable to be effectively attacked by oxygen and ends up contributing greatly to the formation of naphthalene and heavier aromatic species through radical addition processes.

Taking advantage of the successful validation shown in Fig. 3 and interested in probing the interpretation provided by the ROPA, additional simulations were carried out with the two intermediate surrogates (Table 2) to assess the effective impact of di-aromatic and mono-aromatic content on the formation of soot precursors. Fig. 5 compares the simulations from the four different surrogates, in terms of 2-, 3- and 4- aromatic rings (and larger) compounds formation. These profiles

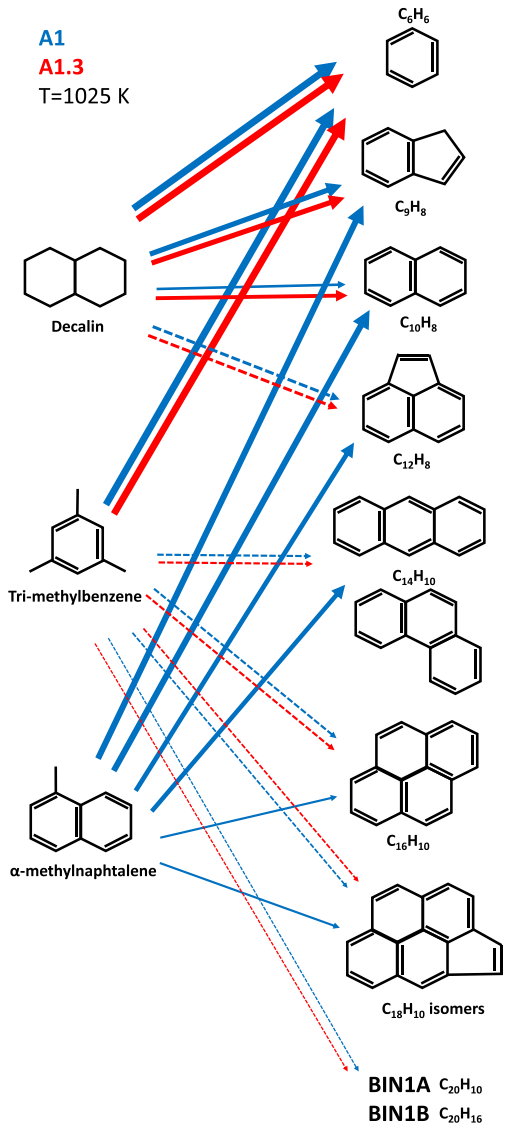

Fig. 4. Schematic representation of the genealogy of PAHs relevant to soot formation. Blue lines refer to Fuel A.1, red lines refer to fuel A1.3. The thickness indicates relative contributions, dashed lines represent indirect contributions (fuel partial decomposition followed by growth by addition.

have been obtained by summing the computed yields of naphthalene, indene, biphenyl, bibenzyl and diphenylmethane in the case of 2-rings PAHs. The major contribution to the total amount of 2-rings PAHs is provided by naphthalene and indene. In an analogous way 3-rings PAHs contain acenaphthylene, phenanthrene, antracene and fluorene while 4-rings are the sum of pyrene, C_{18} and C_{20} lumped PAHs components [19].

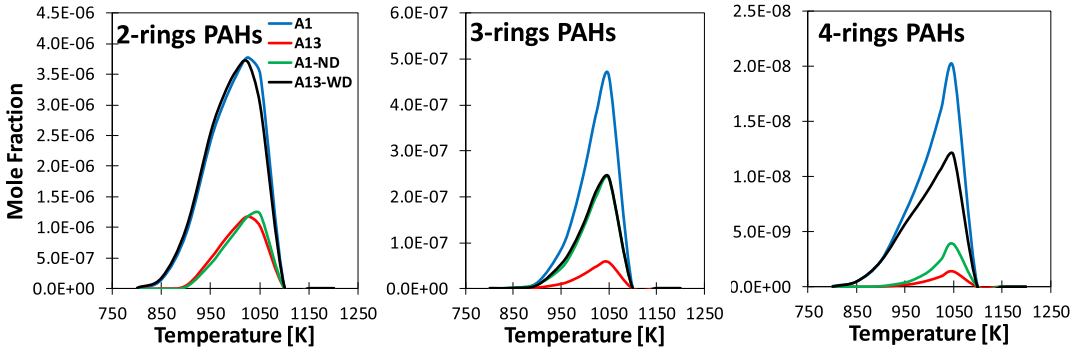

Fig. 5. predicted 2-, 3-, 4-rings PAHs from model simulations with the four different fuel surrogates. Blue: A1, red: A1.3, green: A1-ND, black: A1.3-WD (Table 1).

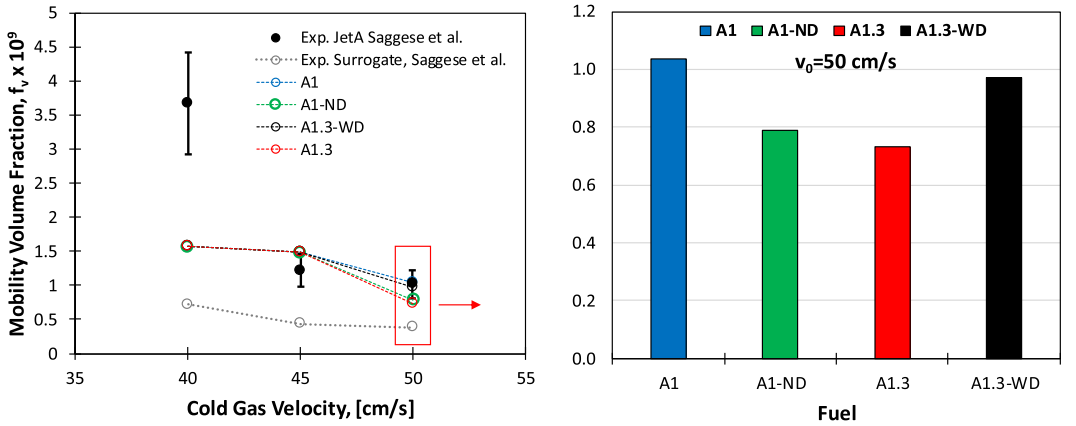

Fig. 6. Comparison of experimental measurements (black symbols) of mobility volume fraction of nascent soot formed in the stretch-stabilizedflame doped with Jet A [26] with model results.

Beside the relatively small absolute concentrations, motivated by the specific conditions at which the DLR flow reactor is operated (i.e. $\varphi = 1.2$, high dilution and relatively low temperatures), the selection of the fuel surrogate has a strong impact. From Fig. 5 it is evident that the removal of 2 mol% of di-aromatic species from the reference A1 surrogate (blue lines) strongly impacts soot precursors formation, decreasing the amount of 2-, 3- and 4-rings species by a factor of ~3, ~2 and ~4, respectively. Trends are covered by the experimental findings up to the 3 ring PAHs while higher species can not be detected due to the bad S/N ratio. Overall, the behavior of the A1-ND surrogate (green lines) approaches, in terms of soot precursors formation, that of the hydro-treated fuel (A1.3) (red lines). As a further proof, the addition of di-aromatic components to the hydro-treated fuel A1.3 leads to a significant increase in PAHs formation. The formation of 2-, 3- and 4-rings aromatics from A1.3-WD fuel (black lines) approaches that observed in the A1 fuel (blue lines).

Saggese et al. [26] recently discussed the variation of the sooting propensity of jet fuels as a function of distillate fractions and examined the validity of a surrogate fuel in reproducing soot production from real fuels. Soot volume fractions were investigated in a series of laminar premixed stretch-stabilized ethylene flames doped with a Jet-A fuel (POSF 10,325, MW = 158.6, H/C = 1.91)), and a surrogate fuel (MURI, MW = 138.7, H/C = 1.96) proposed by Dooley et al. [27]. To extrapolate the effects of the di-aromatic content on soot formation, we compared the results from our surrogate models with the soot volume fraction measurements of Saggese et al. [26]. Temperature and axial velocity profiles are computed in the simulations. Fig. 6 compares mobility volume fraction measurements from [26] and results from model simulations, for the 7260 ppmw jet fuel doping case.

The fuel models here proposed compare reasonably well with the data in [26] but still underestimate the soot volume fraction by 3 folds at the lowest velocity (40 cm/s) or the highest residence times. This could be due to the too slow surface growth reactions in the soot sub-mechanism under these conditions. However, it should be noted how the discrete sectional soot model here used has been validated over a wide range of sooting conditions [19], with different fuels, and possible improvements to the soot module are outside the scope of this paper. Very good agreement is observed for 50 cm/s and 45 cm/s cold gas velocities, conditions that, due to shorter residence times, are more sensitive to the production of nascent soot particles. The difference between the 4 surrogates investigated in this study becomes evident at the highest velocity of 50 cm/s, where the residence time in the flame are the shortest. At this conditions the trend in the sooting tendency previously highlighted for PAHs is conserved (A1.3 < A1-ND < A1.3-WD < A1).

5. Conclusions

This work analyzes the combustion behavior of two jet fuels: a standard, Jet A-1 fuel and a hydro-treated Jet A-1. The two fuels differ mostly in the relative content of aromatics, a feature that reflects in a different propensity to form PAHs and, consequently, soot. New sets of speciation data were measured in a flow reactor, confirming the expected trends in the formation of poly-aromatic species. Fuel models based on a semi-detailed kinetic mechanism and composition based surrogates were validated against the data and used to interpret them. Additional calculations allowed to conclude that fuels containing even a small amount of di-aromatics can produce significant amounts of PAHs, despite having a lower total aromatic content (and a higher H/C ratio). Further calculations extended these findings to soot formation. It was also shown that short contact time exacerbate the compositional effects.

These findings have several important implications on both fuel optimization strategies and surrogate fuels formulation:

1. A simple correlation between the hydrogen content of a fuel and its PAH and particulate formation propensity is not universally applicable. The quality of the aromatic content in the fuel has an important role in determining the sooting behavior.
2. When the goal of a fuel formulation is to reduce particulate emissions, limiting the content in di-aromatics could be the most effective way to curb soot formation.
3. When considering soot formation processes, surrogate fuels used in simulations need to account for the presence of di-aromatic species, even when they are present in small amounts. This issue is closely coupled with the selection of appropriate representative species to be used in the surrogate palette.
4. Based on the simulations, when exploring the fuel effects on sooting propensity, short residence time experiments have an edge in discriminating among fuels. This aspect becomes paramount when the focus is on practical systems, where the gas velocities, compared to the volumes at play, are significant.

Declaration of Competing Interest

The Authors declare that there is no conflict of interest.

Acknowledgments

The authors acknowledge the valuable contribution of Dr. Maira Alves Fortunato (IFP Energies nouvelles, Institut Carnot IFPEN Transports Energy), for providing the GCxGC analysis of the fuels. This work was performed in the context of JetSCREEN, a project funded from the European Union's Horizon 2020 research and innovation program under agreement No. 723525.

Supplementary materials

Supplementary material associated with this article can be found, in the online version, at doi:10.1016/j.proci.2020.06.353.

References

[1] P. Oßwald, M. Köhler, *Rev. Sci. Instrum.* 86 (2015) 105109.
[2] M. Köhler, P. Oßwald, D. Krueger, R. Whitside, *Jove-J Vis. Exp.* (2018) e56965.
[3] T. Bierkandt, P. Oßwald, T. Schripp, M. Köhler, *Combust. Sci. Technol.* 191 (2019) 1499–1519.
[4] T.-C. Chu, Z.J. Buras, P. Oßwald, M. Liu, M.J. Goldman, W.H. Green, *Phys. Chem. Chem. Phys.* 21 (2019) 813–832.
[5] T. Kathrotia, C. Naumann, P. Oßwald, M. Köhler, U. Riedel, *Combust. Flame* 179 (2017) 172–184.
[6] F. Herrmann, P. Oßwald, K. Kohse-Höinghaus, *Proc. Combust. Inst.* 34 (2013) 771–778.
[7] M. Schenk, L. Leon, K. Moshammer, P. Oßwald, T. Zeuch, L. Seidel, F. Mauss, K. Kohse-Höinghaus, *Combust. Flame* 160 (2013) 487–503.
[8] T. Kathrotia, P. Oßwald, M. Köhler, N. Slavinskaya, U. Riedel, *Combust. Flame* 194 (2018) 426–438.
[9] S. Jürgens, P. Oßwald, M. Selinsek, P. Piermartini, J. Schwab, P. Pfeifer, U. Bauder, S. Ruoff, B. Rauch, M. Köhler, *Fuel Process. Technol.* 193 (2019) 232–243.
[10] P. Oßwald, J. Zinsmeister, T. Kathrotia, M. Alves–Fortunato, V. Burger, R. van der Westhuizen, C. Viljoen, K. Lehto, R. Sallinen, K. Sandberg,

M. Aigner, P. Le Clercq, M. Köhler, *In Prep. Fuel* (2020).
[11] A. Violi, S. Yan, E. Eddings, A. Sarofim, S. Granata, T. Faravelli, E. Ranzi, *Combust. Sci. Technol.* 174 (2002) 399–417.
[12] E. Ranzi, A. Frassoldati, A. Stagni, M. Pelucchi, A. Cuoci, T. Faravelli, *Int. J. Chem. Kinet.* 46 (2014) 512–542.
[13] C. Saggese, S. Ferrario, J. Camacho, A. Cuoci, A. Frassoldati, E. Ranzi, H. Wang, T. Faravelli, *Combust. Flame* 162 (2015) 3356–3369.
[14] W. Pejpichestakul, A. Cuoci, A. Frassoldati, M. Pelucchi, A. Parente, T. Faravelli, *Combust. Flame* 205 (2019) 135–146.
[15] W. Pejpichestakul, A. Frassoldati, A. Parente, T. Faravelli, *Combust. Sci. Technol.* 191 (2019) 1473–1483.
[16] W.K. Metcalfe, S.M. Burke, S.S. Ahmed, H.J. Curran, *Int. J. Chem. Kinet.* 45 (2013) 638–675.
[17] S.M. Burke, U. Burke, R. Mc Donagh, O. Mathieu, I. Osorio, C. Keesee, A. Morones, E.L. Petersen, W. Wang, T.A. DeVerter, *Combust. Flame* 162 (2015) 296–314.
[18] G. Bagheri, E. Ranzi, M. Pelucchi, A. Parente, A. Frassoldati, T. Faravelli, *Combust. Flame* 212 (2020) 142–155.
[19] W. Pejpichestakul, E. Ranzi, M. Pelucchi, A. Frassoldati, A. Cuoci, A. Parente, T. Faravelli, *Proc. Combust. Inst.* 37 (2019) 1013–1021.
[20] M. Pelucchi, C. Cavallotti, A. Cuoci, T. Faravelli, A. Frassoldati, E. Ranzi, *React. Chem. Eng.* 4 (2019) 490–506.
[21] S. Dooley, S.H. Won, F.L. Dryer, in: Computer Aided Chemical Engineering, Elsevier, 2019, pp. 513–602.
[22] D. Krüger, P. Oßwald, M. Köhler, P. Hemberger, T. Bierkandt, T. Kasper, *Proc. Combust. Inst.* 37 (2019) 1563–1570.
[23] T. Schripp, B. Anderson, E.C. Crosbie, R.H. Moore, F. Herrmann, P. Oßwald, C. Wahl, M. Kapernaum, M. Köhler, P. Le Clercq, *Environ. Sci. Technol.* 52 (2018) 4969–4978.
[24] T. Kathrotia, U. Riedel, *Fuel* 261 (2020) 116482.
[25] A. Cuoci, A. Frassoldati, T. Faravelli, E. Ranzi, *Comput. Phys. Commun.* 192 (2015) 237–264.
[26] C. Saggese, A.V. Singh, X. Xue, C. Chu, M.R. Kholghy, T. Zhang, J. Camacho, J. Giaccai, J.H. Miller, M.J. Thomson, *Fuel* 235 (2019) 350–362.
[27] S. Dooley, S.H. Won, J. Heyne, T.I. Farouk, Y. Ju, F.L. Dryer, K. Kumar, X. Hui, C.-J. Sung, H. Wang, *Combust. Flame* 159 (2012) 1444–1466.